INVESTIGATION ON TEMPERATURE CONTROL IN THE SPS PROCESS WITH TITANIUM ALUMINIDES

Bernd-Arno BEHRENS, Adrian HEYMANN

Leibniz University Hannover, Institute of Forming Technology and Machines, Garbsen, Germany, EU;
heymann@ifum.uni-hannover.de, behrens@ifum.uni-hannover.de

https://doi.org/10.37904/metal.2021.4221

Abstract

Spark Plasma Sintering (SPS) or Field-Assisted Sintering Technique (FAST) is a powder metallurgical (PM) heat-assisted process, where loose metal powder is pressed to a compact. Powders, which are difficult to consolidate, can be processed much more efficiently than within the conventional PM process route, i.e. die pressing followed by sintering. However, temperature measurement in the SPS process is challenging since it can only be done on the die surface or within the die wall without influencing the process. In case of γ-based Titanium aluminide (TiAl) powders, a suitable sintering temperature allows for a modification of the three grain morphologies lamellar, equiaxed and duplex, and thus for the mechanical properties to be selectively adjusted. In this study, temperature control during the SPS process is investigated using the commercially available pre-alloyed TiAl48-2Cr-2Nb (GE48) powder. For this purpose, temperature measurement with thermocouples and a pyrometer is considered. Furthermore, the influences of graphite and boron nitride lubricants or rather release agents and insulators on the temperature profile are investigated. The evaluation is carried out based on microstructure analysis and hardness measurements. The results show that a suitable temperature control of the process is possible. In addition, it seems that the choice of release agent has a significant influence on the temperature and thus on microstructure and mechanical properties.

Keywords: Spark Plasma Sintering, powder metallurgical process, TiAl powder

1. INTRODUCTION

γ-based titanium aluminides (γ-TiAl) have a high application potential in the automotive and aerospace industries due to their high stiffness, good heat resistance and high specific strength as well as good corrosion resistance and low density, 3.9 - 4.2 g/cm³ [1]. This allows them to be used as a substitute for titanium- or nickel-based alloys while reducing the weight of a component. However, they are difficult to process due to their brittleness [2], which is why the SPS technique is often used [3].

SPS or rather FAST belongs to the in situ pressure-assisted sintering techniques and is characterised by uniaxial pressure application, low voltage and a high density current [4]. The high density current is induced via the tool and acts as a heat source due to the Joule effect. The heat generation depends on the electrical resistance of the tool and the sample. If the sample has a higher electrical resistance, the heat is generated there; otherwise, it is generated in the tool, consisting of die and punches [5]. The tool is usually made of graphite, which is why heating rates of 1000 K/min can be realised while maximum axial pressures are limited to about 150 MPa [5,6]. The adjustment of pressure and temperature enables the targeted setting of the degree of compaction and microstructure and thus the mechanical properties of the compact [5].However, temperature control is an enormous challenge, as temperature measurement directly in the powder conflicts with the production of a perfect compact. Guyon et al. [7] and Liu et al. [3] measured the temperature exclusively with a pyrometer at the die wall, while Lagos et al. [8] measured the temperature inside the punch. In both cases, the actual temperature of the powder is unknown. Couret et al. [9] and Trzaska et al. [10] deduced the actual

temperature during the process from the final microstructure of the compact. However, using this method, it is unclear at the beginning of the process which temperature is necessary at the respective measuring point to obtain the desired result. Molénat et al. [6] and Voisin et al. [11] used FEM calculation to determine the temperature of the powder. Nevertheless, the simplifications made, such as a temperature-independent density, falsify the results. Meanwhile, a more accurate method was used by Martins et al. [5] by measuring the temperature at the stamp surface and in the powder. This allowed them to calculate a correction factor, which could be used to infer the temperature of the powder from the temperature of the punch surface. However, the location of the temperature measurement was not specified, although this would be crucial, as the temperature distribution inside the powder is inhomogeneous during the process [9].

In this study, the temperature control in the SPS process is investigated using the example of commercially available pre-alloyed γ-TiAl powder. The aim is to be able to control the desired process temperature using a suitable reference measurement in the powder. In addition, the influence of different release agents and the use of insulations is investigated, as both should have a major impact on temperature distribution, yet were not considered in the above-mentioned studies. The results are evaluated by means of microstructure investigations and hardness measurements.

2. MATERIALS AND METHODS

The tests were carried out on a sintering press DSP 507 by Dr. Fritsch using TiAl48-2Cr-2Nb (GE48) powder, with a particle size of 45 to 150 µm and a melting temperature of 1510 °C. The powder was produced by the Electrode Induction Melting Gas Atomization process (EIGA) and classified under argon gas. The powder consists of 59.6 wt% Ti, 33 wt% Al, 2.6 wt% Cr and 4.8 wt% Nb. The experimental setup is shown in **Figure 1** on the left. The tool material used was graphite grade 2333 from Mersen Corporate Services SAS. It was additionally covered with a carbon-bonded carbon fibre (CBCF) insulation to reduce heat dissipation (not depicted).

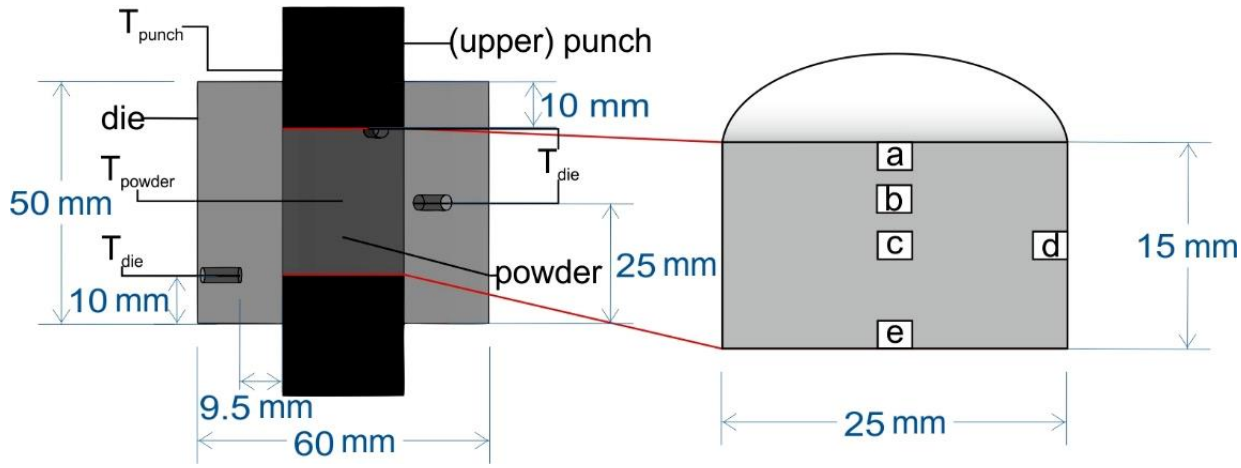

Figure 1 Experimental setup (left) and positions of the morphology images a to e in the sample (right)

Initially, all contact surfaces between the powder and the tool were sprayed with a lubricant or rather release agent. After the spray had dried, the bottom of the die was closed with a punch, the powder was filled in and the top of the die was closed with another punch. In each case, 29.23 g of powder were filled in, theoretically resulting in a cylindrical compact with a diameter of 25 mm and a height of 15 mm at 100 % compression. In the next step, the powder was pre-compacted on a hydraulic hand press, with both punches protruding equally from the die to ensure that the powder can be heated evenly. The temperature was controlled by three type K thermocouples, which were inserted into 8 mm deep holes in the die wall at 9.5 mm from the powder cavity at 10, 25 and 40 mm axial heights at 120° to each other. The temperature T_{die} mentioned in this report refers to

the maximum measured value of these thermocouples. The temperature of the upper punch T_{punch} was observed separately with a pyrometer, which was aligned with the upper punch about 2 mm above the die. As the powder is compacted in the sintering process, the punches move slowly into the die, so that the position of the pyrometer has to be corrected manually several times. Therefore, the pyrometer only gives a tendency of the punch temperature. All tests were carried out under fine vacuum at an axial punch pressure of 30 MPa. The heating rate was slowed down with increasing temperature to enable homogeneous heating of the powder. Based on T_{die}, the heating rate was 60 K/min up to 600 °C, 30 K/min up to 900 °C, 20 K/min up to 1000 °C, 10 K/min up to 1100 °C and 5 K/min up to 1170 °C. The experimental design is shown in **Table 1**. During tests 1 to 3, graphite was used as release agent. In test 1, the actual powder temperature T_{powder} was measured in the centre of the sample. This was used to determine a correction factor with which T_{powder} could be inferred from T_{die} in the subsequent tests. Therefore, the middle thermocouple hole was re-drilled up to the cavity in order to radially insert a type K thermocouple through the hole into the centre of the powder. The run was carried out until the thermocouple failed at T_{powder}= 1200 °C. The aim of test 2 was to set a duplex microstructure at T_{powder} = 1300 °C in the centre of the sample with the help of the previously determined correction factor. Since the temperature is inhomogeneous over the height of the sample [2], in test 3, ceramic discs with a thickness of 4 mm made of Alsint 99.7 (Al_2O_3) were used as electrical and thermal insulators [12] between the punches and the powder in order to achieve a more homogeneous temperature distribution. Since this material is very susceptible to thermal shock, a heating rate of 5 K/min was not to be exceeded when using it. In test 4, the release agent was changed to boron nitride with the aim of reproducing the potential effect of the ceramic discs while allowing higher heating rates. In order to quantify the influence of the release agent on the microstructure and thus the temperature distribution in the sample, the punch faces were sprayed with graphite in the last tests 5 and 6, while the other contact surfaces between powder and tool were sprayed with boron nitride. The evaluation was carried out based on microstructural analyses in the positions as shown in **Figure 1** on the right and Vickers hardness measurements (HV1: test load 9.807 N). For this purpose, the samples were prepared metallographically and etched according to Kroll (3 ml HF + 6 ml HNO_3 + 100 ml H_2O).

Table 1 Experimental design

Test	Release agent	Temperature	Insertion of thermocouple in powder	Ceramic insulation
1	graphite	1200 °C (T_{powder})	Through the die	-
2	graphite	1300 °C (T_{powder})	-	-
3	graphite	1150 °C(T_{die})	-	yes
4	boron nitride	1150 °C (T_{die})	-	-
5	boron nitride, graphite	1130 °C (T_{die})	-	-
6	boron nitride, graphite	1170 °C (T_{die})	-	-

3. RESULTS AND DISCUSSION

During the first three tests with graphite as release agent, T_{punch} was approx. 120 °C higher than T_{die}. In test 1, shortly after the start T_{powder} is about 45 °C higher compared to T_{die}. The difference increases to a maximum of 180 °C up to about T_{die}= 600 °C and then settles at 130 °C in the range of T_{powder}= 1000 °C to 1200 °C (**Figure 2**). During the test, T_{punch} is always colder than T_{powder}. The rapid increase can probably be attributed to the high heating rate up to T_{die}= 600 °C. The subsequently decreasing heating rate leads to an increasing temperature homogenization between powder and tool, so that the temperature difference between the two reaches an approximately constant value (130 °C).

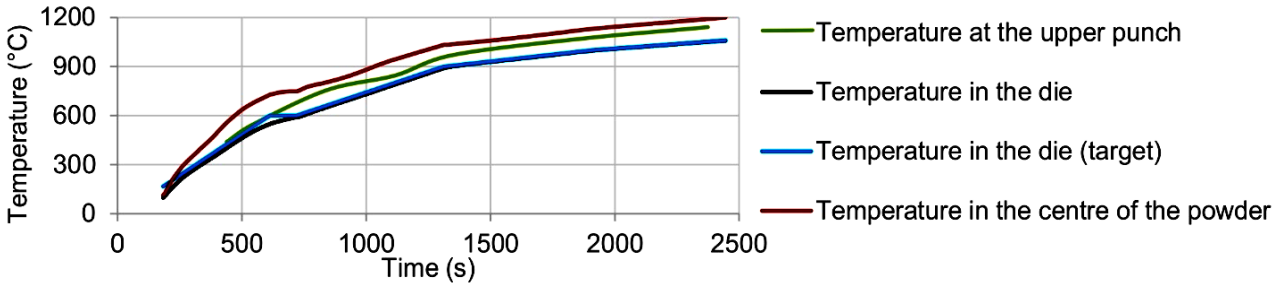

Figure 2 Temperature of die, centre of powder and upper punch vs. process time

In test 2, at T_{die} = 1170 °C, all three microstructural morphologies [13] are evident in the sample, despite initial signs of melting on the sample faces. As a result, a coarse-grained lamellar structure is evident at the end faces, while a duplex structure is present towards the centre of the sample (**Figure 3**). A fine-grained near-γ structure is also visible in the lateral area of the sample [14]. The hardness measurements support the results, as with increasing distance to the end faces, the hardness decreases from about 358±4 HV1 to 298±8 HV1. The results confirm that the temperature in the area of the punch faces is significantly higher compared to T_{die} and to T_{powder}. The likely cause is the much higher electrical resistance of the powder. Consequently, the current only flows through the powder in the face area, heats it up enormously and covers the rest of the distance mainly through the die. The challenge of the resulting heat build-up was met by using ceramic discs in test 3, which were inserted between the punch faces and the powder. The discs act as thermal and electrical insulators that do not transmit the current to the powder [15]. This, together with the slow heating rate, then leads to a more homogeneous temperature distribution within the sample and to a smaller temperature difference between T_{powder} and T_{die}. As a result, a near-γ structure with a uniform hardness of about 255±11 HV1 is formed at T_{die} = 1150 °C.

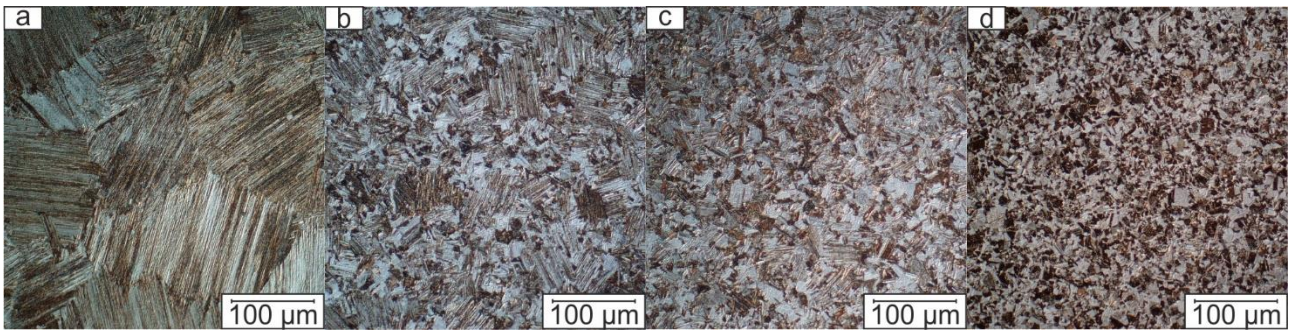

Figure 3 Microstructure in defined positions a, b, c and d according to **Figure 1** (right) of a sample sintered at T_{die} = 1170 °C with graphite as release agent

In test 4, when boron nitride was used as release agent, the punch only became about 40 °C warmer compared to T_{die}. The result is a homogeneous near-γ structure with a hardness of about 280±7 HV1, which is comparable to the use of the ceramic discs. In contrast to graphite, boron nitride acts more as an electrical insulator [16], so that to a small extent the current flows evenly through the powder, but mainly through the tool. Hence, an effect similar to the use of ceramic discs is achieved, with the difference that higher heating rates can be used. In order to direct the current flow mainly through the powder, in test 5 and 6, all contact surfaces between powder and die were sprayed with boron nitride, while only the punch end faces were sprayed with graphite. During these tests, T_{die} corresponds approx. to T_{punch} with a maximum difference of 20 °C. At 1130 °C, a near-γ structure can be seen (**Figure 4**). The measured hardness there is 280±5 HV1. However, a lamellar structure can be seen in the lower sample area. This can be related to the different depths

of the punches inserted in the die. The punch, which is more in contact with the die, experiences less cooling from the relatively cold chamber and heats up more, which leads to a higher temperature.

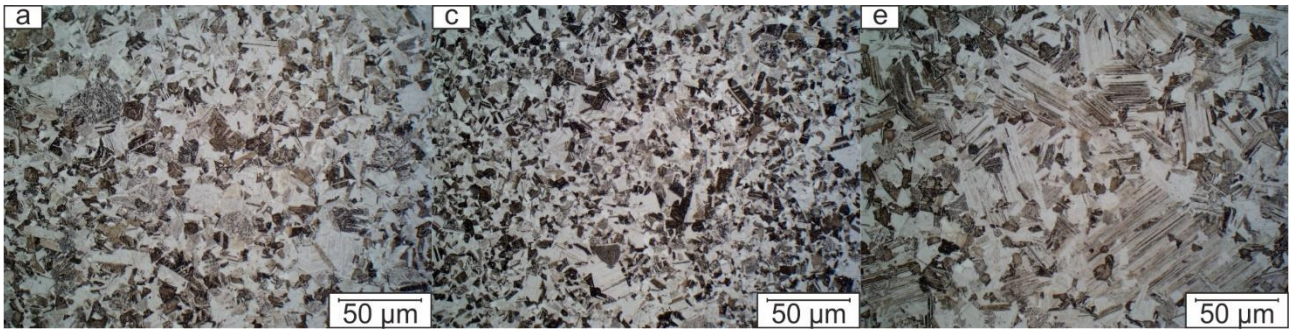

Figure 4 Microstructure in defined positions a, c and e according to **Figure 1** (right) of a sample sintered at T_{die} = 1130 °C with graphite and boron nitride as release agents

In test 6, at 1170 °C, the lower punch was probably also located further inside the die during the process. The overview image in **Figure 5** shows much larger grains on the end faces, which become smaller towards the lateral area and towards the centre of the sample. However, no melting is visible as in test 2. Over the height of the specimen, the hardness decreases from about 291±4 HV1 to 282±1 HV1 from the end faces to the centre, while it is about 280±9 HV1 in the centre over the diameter of the sample.

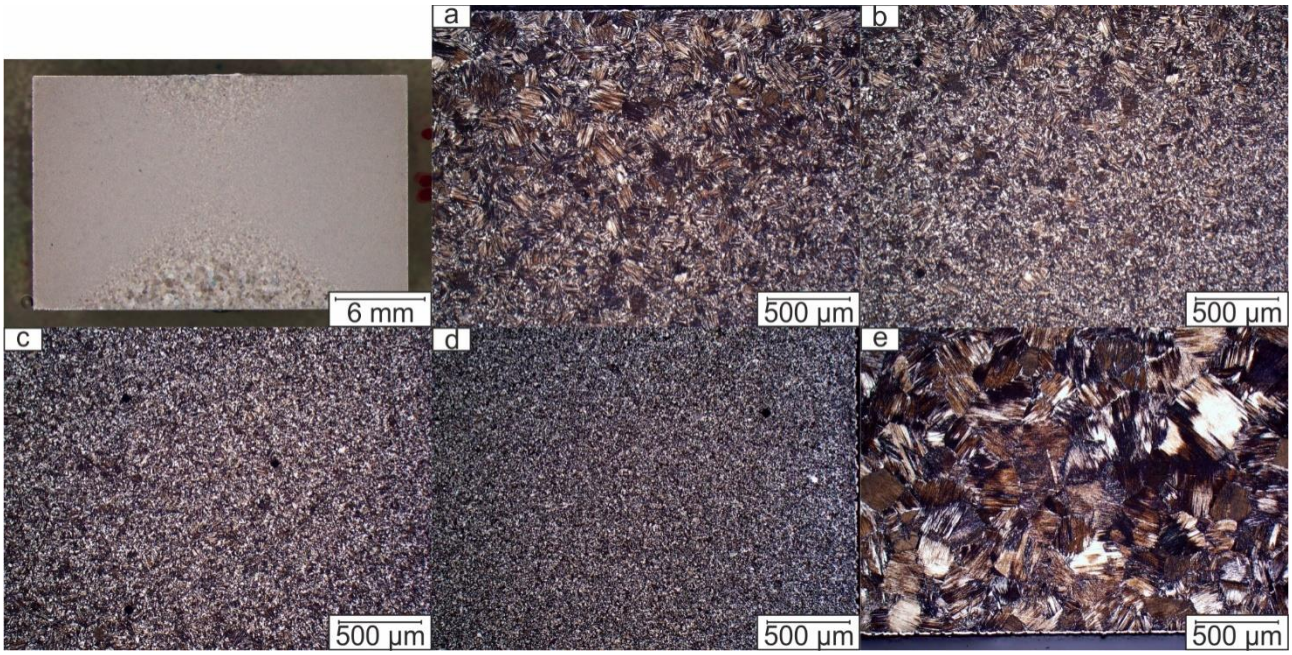

Figure 5 Microstructure in defined positions a, b, c, d and e according to **Figure 1** (right) of a sample sintered at T_{die} = 1170 °C with graphite and boron nitride as release agents

4. CONCLUSION

Within the scope of the investigations, temperature measurements were carried out directly in the powder and at different positions of the tool during the SPS process. It was found that when exclusively graphite is used as release agent, the punches become much warmer than the die and the powder. In this case, T_{powder} was 130 °C higher and T_{punch} was 120 °C higher compared to T_{die}. Heat builds up between the punch face and the powder, which at T_{die} = 1170 °C leads to melting of the powder on the punches. The influence of the heat build-

up could be minimised by using ceramic discs at the expense of a significantly higher process time. The large temperature difference between the punch face and the powder was reduced by a modified release agent strategy. For this purpose, the punch faces were sprayed with graphite, while the other contacts between powder and tool were sprayed with boron nitride. Since the latter acts as an electrical insulator, more of the current flow was able to pass through the powder via the punches, causing it to heat up more homogeneously and preventing it from melting at T_{die} = 1170 °C. However, the microstructure continues to vary across the sample height due to temperature gradients within the sample, which is supported by the hardness values. A reduced sample height or a better electrically insulating release agent could remedy the situation.

ACKNOWLEDGEMENTS

Funded by the Deutsche Forschungsgemeinschaft (DFG, German Research Foundation) – Project-ID 394563137 – SFB 1368

REFERENCES

[1] GERLING, R., CLEMENS, H., SCHIMANSKY, F.P. Powder metallurgical processing of intermetallic gamma titanium aluminides. *Advanced Engineering Materials*. 2004, vol. 6, no. 12, pp. 23–38.

[2] YAMAGUCHI, M., INUI, H., ITO, K. High-temperature structural intermetallics. *Acta Materialia*. 2000, vol. 48, no. 1, pp. 307–322.

[3] LIU, H.-W., BISHOP, D.P., PLUCKNETT, K.P. Densification behaviour and microstructural evolution of Ti-48Al consolidated by spark plasma sintering. *Journal of Materials Science*. 2017, vol. 52, no. 1, pp. 613–627.

[4] MAMEDOV, V. Spark plasma sintering as advanced PM sintering method. *Powder Metallurgy*. 2002, vol. 45, no. 4, pp. 322–328.

[5] MARTINS, D., GRUMBACH, F., SIMOULIN, A., SALLOT, P., MOCELLIN, K., BELLET, M., ESTOURNÈS, C. Spark Plasma Sintering of a commercial TiAl 48-2-2 powder: Densification and creep analysis. *Materials Science and Engineering: A*. 2018, vol. 711, pp. 313–316.

[6] MOLÉNAT, G., DURAND, L., GALY, J., COURET, A. Temperature Control in Spark Plasma Sintering: An FEM Approach. *Journal of Metallurgy*. 2010, pp. 1–9.

[7] GUYON, J., HAZOTTE, A., MONCHOUX, J.P., BOUZY, E. Effect of powder state on spark plasma sintering of TiAl alloys. *Intermetallics*. 2013, vol. 34, pp. 94–100.

[8] LAGOS, M.A., AGOTE, I. SPS synthesis and consolidation of TiAl alloys from elemental powders: Microstructure evolution. *Intermetallics*. 2013, vol. 36, pp. 51–56.

[9] COURET, A., MOLÉNAT, G., GALY, J., THOMAS, M. Microstructures and mechanical properties of TiAl alloys consolidated by spark plasma sintering. *Intermetallics*. 2008, vol. 16, no. 9, pp. 1134–1141.

[10] TRZASKA, Z., COURET, A., MONCHOUX, J.-P. Spark Plasma Sintering mechanisms at the necks between TiAl powder particles. *Acta Materialia*. 2016, vol. 118, pp. 100–108.

[11] VOISIN, T., DURAND, L., KARNATAK, N., LE GALLET, S., THOMAS, M., LE BERRE, Y., CASTAGNÉ, J.-F., COURET, A. Temperature control during Spark Plasma Sintering and application to up-scaling and complex shaping. *Journal of Materials Processing Technology*. 2013, vol. 213, no. 2, pp. 269–278.

[12] BEHRENS, B.-A., FISCHER, D., HALLER, B., RASSILI, A., KLEMM, H., FLÜß, A., WALKIN, B., KARLSSON, M., ROBELET, M., CUCATTO, A. Introduction of a full automated process for the production of automotive steel parts. In: *Proceedings of the 8th International conference on Semi-solid processing of alloys and composites*, Limassol: S2P 2004, 2004, pp. 77–88

[13] COURET, A., VOISIN, T., THOMAS, M., MONCHOUX, J.-P. Development of a TiAl alloy by spark plasma sintering. *JOM*. 2017, vol. 69, no. 12, pp. 2576–2582.

[14] VANMEENSEL, K., LAPTEV, A., HENNICKE, J., VLEUGELS, J., VANDERBIEST, O. Modelling of the temperature distribution during field assisted sintering. *Acta Materialia*. 2005, vol. 53, no. 16, pp. 4379–4388.

[15] SUN, Y., KULKARNI, K., SACHDEV, A.K., LAVERNIA, E.J. Synthesis of γ-TiAl by reactive Spark Plasma Sintering of cryomilled Ti and Al powder blend: Part II: Effects of Electric Field and Microstructure on Sintering Kinetics. *Metallurgical and Materials Transactions A*. 2014, vol. 45, no. 6, pp. 2759–2767.

[16] PAULING, L. The structure and properties of graphite and boron nitride. In: *Proceedings of the National Academy of Sciences of the United States of America*. 1966, vol. 56, no. 6, pp. 1646–1652.